4322 *Organometallics* **2003,** *22,* 4322−4326

A Combined Experimental and Theoretical Study Examining the Binding of *N*-Heterocyclic Carbenes (NHC) to the Cp*RuCl (Cp* = η^5-C$_5$Me$_5$) Moiety: Insight into Stereoelectronic Differences between Unsaturated and Saturated NHC Ligands

Anna C. Hillier,[†] William J. Sommer,[†] Ben S. Yong,[†] Jeffrey L. Petersen,[‡]
Luigi Cavallo,[§] and Steven P. Nolan*,[†]

Department of Chemistry, University of New Orleans, New Orleans, Louisiana 70148,
Department of Chemistry, West Virginia University, Morgantown, West Virginia 26506, and
Dipartimento di Chimica, Università di Salerno, Baronissi (SA) I-84081, Italy

Received July 4, 2003

Combined solution calorimetric and quantum mechanics studies of reactions involving saturated and unsaturated *N*-heterocyclic carbene (NHC) ligands show that the difference in their relative bond dissociation energies is very small (1 kcal·mol^{-1}). Structural and computational studies reveal small metric parameter differences. These observations in conjunction with relative reactivity profiles of NHC-modified ruthenium-based olefin metathesis catalysts suggest that very small changes in the donor properties of the NHC ligands can translate into significant differences in catalytic properties.

Introduction

The now widely used olefin metathesis assembly strategy owes its general acceptance in the organic community mainly to the discovery of highly active, well-defined catalysts of both ruthenium and molybdenum.[1−5] The neutral 16-electron ruthenium benzylidene complex RuCl$_2$(=C(H)Ph)(PCy$_3$)$_2$ (Grubbs' catalyst, **1**)[6,7] has proven to be a powerful catalytic mediator in a variety of olefin metathesis reactions, as have its second generation derivatives modified with *N*-heterocyclic carbenes RuCl$_2$(=C(H)Ph)(PCy$_3$)(IMes) (**2**)[8−12] (IMes = 1,3-bis(2,4,6-trimethylphenyl) imidazol-2-ylidene) and RuCl$_2$(=C(H)Ph)(PCy$_3$)(SIMes) (**3**)[13] (SIMes = 1,3-bis(2,4,6-trimethylphenyl)-4,5-dihydroimidazol-2-ylidene) (Figure 1).

These reactions include ring-closing metathesis (RCM),[14−24] ring-opening metathesis polymerization (ROMP),[25,26] cross metathesis (CM),[27−33] intramolecular

---

[*] Corresponding author. E-mail: snolan@uno.edu.

[†] University of New Orleans.

[‡] West Virginia University.

[§] Università di Salerno.

(1) Trnka, T. M.; Grubbs, R. H. *Acc. Chem. Res.* **2001**, *34*, 18−29.

(2) Grubbs, R. H.; Chang, S. *Tetrahedron* **1998**, *54*, 4413−4450, and references therein.

(3) Ivin, K. *J. Mol. Catal. A Chem*. **1998**, *133*, 1−16.

(4) Randall, M. L.; Snapper, M. L. *J. Mol. Catal. A Chem*. **1998**, *133*, 29−40.

(5) For a comprehensive review, see: Ivin, K.; Mol, J. C. *Olefin Metathesis and Metathesis Polymerization*; Academic Press: London, 1997.

(6) Schwab, P.; France, M. B.; Ziller, J. W.; Grubbs, R. H. *Angew. Chem., Int. Ed. Engl.* **1995**, *34*, 2039−2041.

(7) Schwab, P.; Grubbs, R. H.; Ziller, J. W. *J. Am. Chem. Soc.* **1996**, *118*, 100−110.

(8) Huang, J.; Stevens, E. D.; Nolan, S. P.; Petersen, J. L. *J. Am. Chem. Soc.* **1999**, *121*, 2674−2678.

(9) Scholl, M.; Trnka, T. M.; Morgan, J. P.; Grubbs, R. H. *Tetrahedron Lett.* **1999**, *40*, 2247−2250.

(10) Weskamp, T.; Kohl, F. J.; Hieringer, W.; Gleich, D.; Herrmann, W. A. *Angew. Chem., Int. Ed.* **1999**, *38*, 2416−2419.

(11) Jarfapour, L.; Nolan, S. P. *Organometallics* **2000**, *19*, 2055−2957.

(12) Jarfapour, L.; Hillier, A. C.; Nolan, S. P. *Organometallics* **2002**, *21*, 442−444.

(13) Scholl, M.; Ding, S.; Lee, C. W.; Grubbs, R. H. *Org. Lett.* **1999**, *1*, 953−956.

(14) Heck, M.-P.; Baylon, C.; Nolan, S. P.; Mioskowski, C. *Org. Lett.* **2001**, *3*, 1989−1991.

(15) Boyer, F.-D.; Hanna, I.; Nolan, S. P. *J. Org. Chem.* **2001**, *66*, 4094−4096.

(16) Wagner, J.; Martin Cabrejas, L. M.; Grossmith, C. E.; Papageorgiou, C.; Senia, F.; Wagner, D.; France, J.; Nolan, S. P. *J. Org. Chem.* **2000**, *65*, 9255−9260.

(17) Fürstner, A.; Thiel, O. R.; Ackermann, L.; Schanz, H.-J.; Nolan, S. P. *J. Org. Chem.* **2000**, *65*, 2204−2207.

(18) Briot, A.; Bujard, M.; Gouverneur, V.; Nolan, S. P.; Mioskowski, C. *Org. Lett.* **2000**, *2*, 1517−1519.

(19) Hyldtoft, L.; Madsen, R. *J. Am. Chem. Soc.* **2000**, *122*, 8444−8452.

(20) Fürstner, A.; Thiel, O. R.; Kindler, N.; Bartkowska, B. *J. Org. Chem.* **2000**, *65*, 7990−7995.

(21) Fürstner, A.; Thiel, O. R.; Ackermann, L. *Org. Lett.* **2001**, *3*, 449−451.

(22) Fürstner, A.; Thiel, O. R.; Blanda, G. *Org. Lett.* **2000**, *2*, 3731−3734.

(23) Benningshof, J. C. J.; Blaauw, R. H.; van Ginkel, A. E.; Rutjes, F. P. J. T.; Fraanje, J.; Goubitz, K.; Schenk, H.; Hiemstra, H. *Chem. Commun.* **2000**, 1465−1466.

(24) Fürstner, A.; Ackermann, L.; Gabor, B.; Goddard, R.; Lehmann, C. W.; Mynott, R.; Stelzer, F.; Thiel, O. R. *Chem.; A Eur. J.* **2001**, *7*, 3236−3253.

(25) Hamilton, J. G.; Frenzel, U.; Kohl, F. J.; Weskamp, T.; Rooney, J. J.; Herrmann, W. A.; Nuyken, O. *J. Organomet. Chem.* **2000**, *606*, 8−12.

(26) Bielawski, C. W.; Grubbs, R. H. *Angew. Chem., Int. Ed.* **2000**, *39*, 2903−2906.

(27) Choi, T.-L.; Chatterjee, A. K.; Grubbs, R. H. *Angew. Chem., Int. Ed.* **2001**, *40*, 1277−1279.

(28) Kitamura, T.; Sato, Y.; Mori, M. *Chem. Commun.* **2001**, 1258−1259.

(29) Smulik, J. A.; Diver, S. T. *Org. Lett.* **2000**, *2*, 2271−2274.

(30) Ahmed, M.; Arnauld, T.; Barrett, A. G. M.; Braddock, D. C.; Flack, K.; Procopiou, P. A. *Org. Lett.* **2000**, *2*, 551−553.

(31) Stragies, R.; Voigtmann, U.; Blechert, S. *Tetrahedron Lett.* **2000**, *41*, 5465−5468.

(32) Chaterjee, A. K.; Morgan, J. P.; Scholl, M.; Grubbs, R. H. *J. Am. Chem. Soc.* **2000**, *122*, 3783−3784.

(33) Chaterjee, A. K.; Grubbs, R. H. *Org. Lett.* **1999**, *1*, 1751−1753.

10.1021/om034016k CCC: $25.00

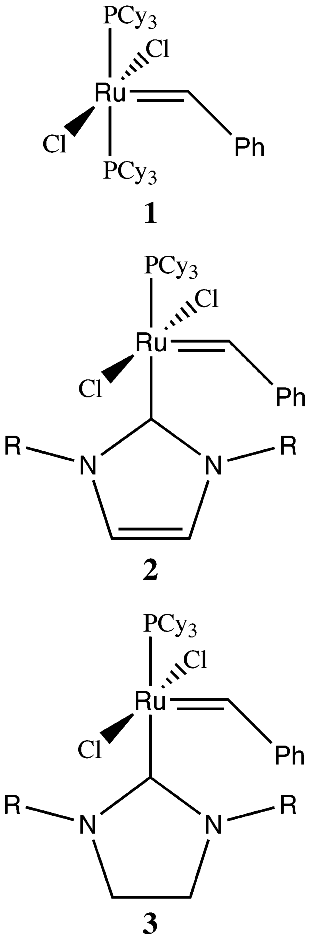

R = 2,4,6-trimethylphenyl (mesityl)

Figure 1. First- and second-generation ruthenium olefin metathesis catalysts.

R	L	R	L
2,4,6-trimethylphenyl	IMes	2,4,6-trimethylphenyl	SIMes
2,6-diisopropylphenyl	IPr	2,6-diisopropylphenyl	SIPr

Figure 2. *N*-Heterocyclic carbene ligands.

enyne cycloisomerization,[24] and their combinations. Nucleophilic *N*-heterocyclic carbenes (NHC) are increasingly attractive alternatives to phosphine ligands in organometallic catalytic systems (IMes, SIMes, IPr, and SIPr are shown in Figure 2). This is due to both their ease of preparation (via air-stable imidazolium salt precursors) and the greater degree of thermal stability they impart to catalytic systems, which usually translates in improved catalytic activity.[34]

Complexes **2** and **3**, for example, exhibit higher activity than **1** at elevated temperatures and are stable at these temperatures (**1** is thermally unstable and decomposes upon thermal treatment), enabling access to previously unattainable olefin metathesis activity. A related ruthenium−indenylidene complex also displays this improved thermal stability behavior once modified with a NHC. This latter complex has successfully been used as an alternative to the ruthenium−benzylidene complexes in olefin metathesis.[35−41]

The subtle steric and electronic differences within the NHC class of ligand remain relatively unquantified. Calorimetric studies have compared the binding enthalpies of a number of phosphines and NHC ligands in the Cp*Ru(L)Cl system (Cp* = η^5-C$_5$Me$_5$; L = NHC, phosphine) and demonstrated that the unsaturated NHC ligands bind more strongly than the widely used PCy$_3$ and P^{i}Pr$_3$ ligands. The exception to this is the very sterically congested IAd ligand, bearing 1-adamantyl substituents on the nitrogens.[42] The NHC ligand IMes, for example, has a relative bond dissociation energy (BDE) of 15.6 kcal·mol^{-1} compared to 10.5 kcal·mol^{-1} for PCy$_3$. To date, however, no studies have been conducted on the saturated analogues of these ligands, and the enhancement of catalytic activity of complexes bearing NHC has been attributed to their greater donor ability without supporting quantitative evidence.[43] We report here calorimetric and structural studies on the SIMes and SIPr NHC ligands (SIPr = 1,3-bis(2,6-diisopropylphenyl)-4,5-dihydroimidazol-2-ylidene) in the Cp*Ru(L)Cl system (L = SIMes, **4**; L = SIPr, **5**). To provide a more complete investigation of these aspects, density functional theory calculations are also reported here on both structures of the Cp*Ru(L)Cl complexes and energies of binding of NHC ligands to the Ru atom.

Results and Discussion

The versatile starting material [Cp*RuCl]$_4$ (**6**) reacts with tertiary phosphines[44] and sterically demanding NHC ligands[42] to afford deep blue, coordinatively unsaturated complexes of general formula Cp*Ru(L)Cl. Reaction of **6** with 4 equiv of SIMes or SIPr in THF yielded deep blue solutions from which complexes **4** and **5** were isolated in 69% and 90% yields, respectively, after workup (eq 1).

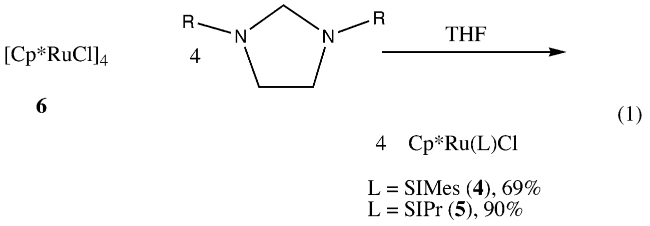

The reactions depicted in eq 1 were rapid and quantitative by ^{1}H NMR spectroscopy and were therefore suitable for calorimetric investigation using a

---

[34] Huang, J.; Schanz, H.-J.; Stevens, E. D.; Nolan, S. P. *Organometallics* **1999**, *18*, 5375−5380.

[35] Jarfapour, L.; Schanz, H.-J.; Stevens, E. D.; Nolan, S. P. *Organometallics* **1999**, *18*, 5416−5419.

[36] Jarfapour, L.; Nolan, S. P. *Adv. Organomet. Chem.* **2001**, *46*, 181−222, and references therein.

[37] Fürstner, A.; Grabowski, J.; Lehmann, C. W. *J. Org. Chem.* **1999**, *64*, 8275−8280.

[38] Fürstner, A.; Thiel, O. R. *J. Org. Chem.* **2000**, *65*, 1738−1742.

[39] Fürstner, A.; Radkowski, K. *Chem. Commun.* **2001**, 671−672.

[40] Fürstner, A.; Radkowski, K.; Wirtz, C.; Goddard, R.; Lehmann, C. W.; Mynott, R. *J. Am. Chem. Soc.* **2002**, *124*, 7061−7069.

[41] Fürstner, A.; Guth, O.; Duffels, A.; Seidel, G.; Liebl, M.; Gabor, B.; Mynott, R. *Chem.−A Eur. J.* **2001**, *7*, 4811−4820.

[42] Huang, J.; Schanz, H.-J.; Stevens, E. D.; Nolan, S. P. *Organometallics* **1999**, *18*, 2370−2375.

Table 1. Enthalpies of Ligand Substitution and Relative Bond Disruption Enthalpies (kcal·mol^{-1}) for the Reaction

$$[\mathrm{Cp^*RuCl}]_4 + 4\ \mathrm{L} \xrightarrow[\mathrm{THF}]{} 4\ \mathrm{Cp^*Ru(L)Cl}$$

L	$-\Delta H_{\mathrm{rxn}}$	relative BDE (experimental)	relative BDE (theoretical)[c]
SIMes	67.1(0.3)	16.8	19.2
IMes	62.6(0.2)[a]	15.6	19.2
SIPr	48.5(0.4)	12.1	10.9
IPr	44.5(0.4)[b]	11.1	11.6
SITol			27.5
ITol	75.3(0.4)[a]	18.8	26.2
PCy_3	41.9(0.2)[b]	10.5	–

[a] Taken from ref 8. [b] Taken from ref 36. [c] In the gas phase.

calorimetric protocol similar to that previously reported.[45] Enthalpies of reaction of −67.1(0.3) and −48.5 (0.4) kcal·mol^{-1} were measured for complexes **4** and **5**, respectively, when 4 equiv of the ligand was reacted under anaerobic conditions with 1 equiv of **6** in THF at 30 °C. Relative bond dissociation energies (BDEs) were calculated by dividing the reaction enthalpy by the number of bonds formed (four). These values can be compared with the reaction enthalpies for the reaction between **6** and IMes (to form **7**), IPr (to form **8**), and PCy_3 (Table 1).

Contrary to expectation, in this system the differences in reaction enthalpies between IMes and SIMes in complexes **7** and **4** and IPr and SIPr in complexes **8** and **5** were very small and yielded a difference in BDE of only +1 kcal·mol^{-1} in each case.

The surprisingly small differences in the experimental reaction enthalpies also emerge from DFT calculations we performed. The calculated BDEs of the NHC ligands, reported in Table 1, are in good semiquantitative agreement with the experimental values. In fact, according to the DFT approach used here, the binding energy of SIMes and IMes is the same, while IPr is even calculated to bind to Cp*RuCl slightly better than SIPr (0.7 kcal·mol^{-1}).

To ascertain the effect of this small difference of the bonding in these complexes, single crystals of both **4** and **5** were studied by X-ray diffraction. The complexes were crystallized by cooling saturated solutions in pentane to −50 °C, yielding small deep blue blocks (in the case of **4**) or needles (for complex **5**). The crystal structures of **4** and **5** are shown in Figures 3 and 4, respectively, and selected bond lengths and angles are shown in Table 2, along with the analogous parameters for the unsaturated carbene complexes **7** and **8**.

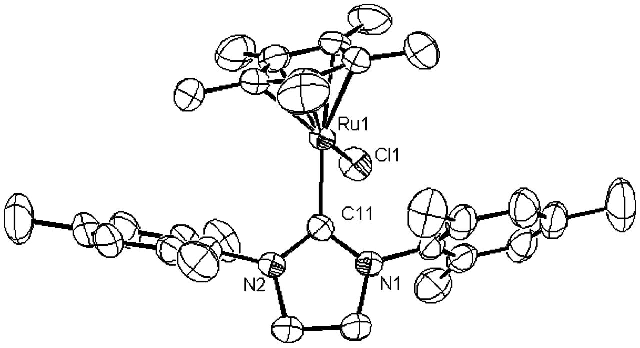

Figure 3. ORTEP plot of Cp*Ru(SIMes)Cl (**4**). Ellipsoids are shown at 50% probability.

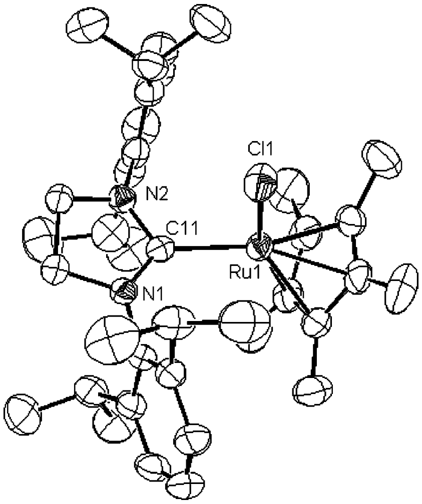

Figure 4. ORTEP plot of Cp*Ru(SIPr)Cl (**5**). Ellipsoids are shown at 50% probability.

Table 2. Selected Bond Lengths (Å) and Angles (deg) for Cp*Ru(L)Cl Complexes (values in parenthesis are from DFT calculations)

ligand	Ru−C	Ru−Cl	Ru−Cp*	C−Ru−Cl	C−Ru−Cp*	Cp*−Ru−Cl
IMes[a]	2.105	2.376	1.766	90.6	140.7	128.6
	(2.086)	(2.387)	(1.799)	(93.4)	(139.9)	(126.7)
SIMes	2.083	2.373	1.772	91.2	140.8	128.0
	(2.076)	(2.386)	(1.806)	(94.3)	(139.9)	(125.8)
IPr[b]	2.086	2.371	1.754	89.3	141.5	129.2
	(2.093)	(2.375)	(1.800)	(89.6)	(143.1)	(127.2)
SIPr	2.087	2.369	1.763	87.2	144.6	128.2
	(2.078)	(2.375)	(1.807)	(89.3)	(144.5)	(126.2)
ITol[a]	2.068	2.340	1.803	94.8	131.9	133.2
	(2.044)	(2.386)	(1.804)	(97.1)	(130.8)	(132.0)
SITol	(2.034)	(2.393)	(1.804)	(97.1)	(130.8)	(132.0)

[a] Taken from ref 8. [b] Taken from ref 36.

There is a small (but statistically significant) difference in the Ru−C$_{\mathrm{carbene}}$ bond length in complexes **4** and **7**, which is consistent with the marginally better electron donor properties of SIMes when compared to IMes, as determined by the solution calorimetry discussed previously. While there appears to be no significant difference in the Ru−C$_{\mathrm{carbene}}$ bond length in complexes **5** and **8**, the Ru−Cp*$_{\mathrm{centroid}}$ distance is longer in **5**, and the Cl−Ru−C$_{\mathrm{carbene}}$ angle smaller. On the basis of our previous work on the $Cp^*Ru(PR_3)Cl$[46] and $Cp^*Ru(PR_3)_2Cl$[47] systems, it may not appear surprising that steric factors play a most important role in the present system. This general observation is corroborated by metrical parameter trends such as the slightly larger Cp*$_{\mathrm{centroid}}$−Ru−C$_{\mathrm{carbene}}$ angle of complexes **5** and **8** when compared to the analogous angles in complexes **4** and **7**. This (along with the greater Cl−Ru−C$_{\mathrm{carbene}}$ angles in the complexes of the mesityl-functionalized carbenes) is consistent with the enhanced steric demand of the SIPr ligand compared to that of SIMes.

---

(43) Cavallo has recently reported a theoretical study offering explanations for the improved reaction profile of **1** versus **2** and **3**. No explanation is however provided for the reaction profile differences of **2** and **3**: Cavallo, L. *J. Am. Chem. Soc.* **2002**, *124*, 8965−8973.

(44) Campion, B. K.; Heyn, R. H.; Tilley, T. D. *Chem. Commun.* **1998**, 278−280.

(45) Serron, S.; Huang, J.; Nolan, S. P. *Organometallics* **1998**, *17*, 534−539.

(46) Luo, L.; Nolan, S. P. *Organometallics* **1994**, *13*, 4781−4786.

(47) Luo, L.; Nolan, S. P. *Organometallics* **1993**, *12*, 4305−4311.

As for the BDE, the structures from DFT calculations are in good semiquantitative agreement with the experimental X-ray structures. This is confirmed by the small rms of the DFT structure of Cp*Ru(SIMes)Cl and Cp*Ru(SIPr)Cl from the corresponding X-ray structure (0.06 and 0.08 Å on all the heavy atoms, respectively). The most relevant geometrical parameters are reported in Table 2 and suggest that the Ru−C distance is shorter in the saturated NHC complexes. This is well in line with the expected better electron donor properties of saturated NHC ligands.

To investigate in more detail the role of the steric bulk of the Me and *i*-Pr substituents, we also calculated the BDE of the NHC ligand in the Cp*Ru(SITol)Cl and Cp*Ru(ITol)Cl complexes. Steric effects should be minimized in these complexes, due to the absence of alkyl substituents in the *ortho* position of the phenyl rings of the NHC ligand. The calculated BDEs are reported in Table 1, while the most relevant geometrical parameters are reported in Table 2. It is clear that the steric bulk of the Me substituents in the IMes- and SIMes-based complexes strongly reduces the BDE, relative to the ITol- and SITol-based complexes. The *i*-Pr substituents in the IPr- and SIPr-based complexes further decrease the BDE. More interestingly, for the less bulky Cp*Ru(ITol)Cl and Cp*Ru(SITol)Cl complexes, the saturated SITol ligand is predicted to bind more strongly than the unsaturated ITol ligand by 1.3 kcal·mol^{-1}, whereas for the bulkier IPr- and SIPr-based complexes, the saturated SIPr ligand binds less strongly than the unsaturated IPr ligand by 0.7 kcal·mol^{-1}. The calculated relative stability of the saturated and unsaturated complexes is affected by the bulkiness of the NHC ligands because shorter Ru−C distances are predicted for the saturated complexes, which of course enhances steric effects. Considering that our computational approach underestimates the differences in the relative BDEs by roughly 1−2 kcal·mol^{-1} (compare the relative experimental and theoretical BDEs for the IMes and SIMes systems, as well as for the IPr and SIPr systems), it is reasonable to estimate that in the absence of steric effects saturated NHC ligands are better donors than the corresponding unsaturated NHC by no more than 2−3 kcal·mol^{-1}.

To quantify the steric factors characterizing these ligands, we measured the amount of volume of a sphere centered on the metal, buried by overlap with atoms of the various NHC ligands, %V_{Bur}. The volume of this sphere would represent the space around the metal atom that must be shared by the different ligands upon coordination. Of course, the bulkier a specific ligand, the larger the amount of that sphere will be occupied by the ligand, i.e., greater %V_{Bur}. To have an aseptic estimate of the bulkiness of the various ligands, we examined the DFT optimized geometries of the free ligands and positioned the putative metal atom at 2 Å from the coordinating C or P atom (for NHC and PCy$_3$ ligands, respectively). A graphical representation of this geometrical analysis is reported in Figure 5. Test calculations suggested that 3 Å is a reasonable radius for the sphere centered on the metal. Incidentally, 3 Å is roughly the distance between the N atoms and the putative metal atom. Clearly, different values for the radius of this sphere would result in different values of %V_{Bur}. A compilation of %V_{Bur} values is presented in Table 3.

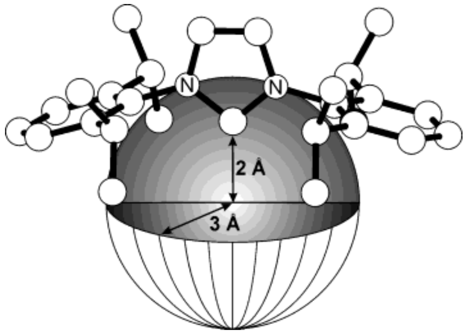

Figure 5. Sphere dimensions for steric parameter determination (%V_{Bur}) of NHC ligands.

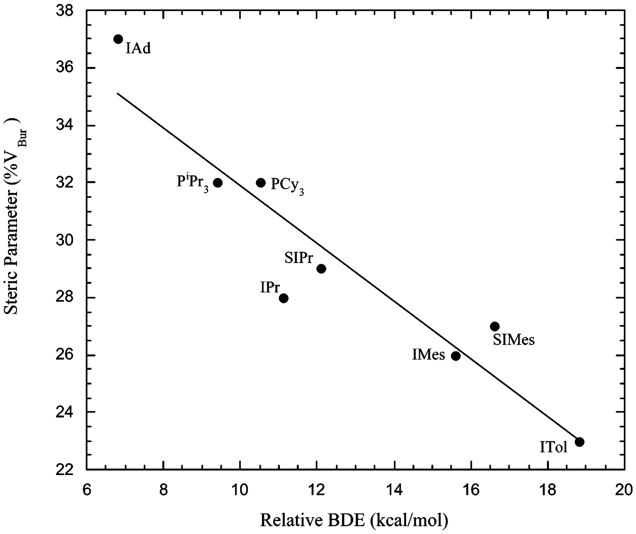

Figure 6. Relative bond disruption enthalpy (kcal/mol) vs steric parameter (%V_{Bur}) in the Cp*Ru(L)Cl system (slope: −1.01; *R*: 0.94).

Table 3. Steric Parameters Associated with Selected NHC and Sterically Demanding PR$_3$ Ligands

ligand	%V_{Bur}
ITol	23
IMes	26
SIMes	27
IPr	28
SIPr	29
P^{i}Pr$_3$	32
PCy$_3$	32
IAd	37

This simple model is only a starting point to try to understand the steric requirements of nonsymmetric NHC ligands. It enables comparisons with more symmetrical tertiary phosphine ligands.

Since there is a preponderant steric factor in the Cp*Ru(L)Cl and Cp*Ru(L)$_2$Cl systems,[46,47] we were interested in testing our initial steric factor values in a simple steric factor versus enthalpy relationship. The experimental BDEs reported in Table 1 are plotted versus %V_{Bur}, and the relationship is presented in Figure 6. The data show a linear correlation between the experimental BDEs and the %V_{Bur}, which suggests that the BDEs are essentially controlled by the steric requirements of the ligands.

Conclusions

Calorimetric and structural investigations have allowed us to compare the saturated NHC ligands SIMes and SIPr with their unsaturated analogues IMes and IPr in terms of both steric bulk and electron donor ability in the Cp*Ru(L)Cl complexes. The data demonstrate that SIMes is a better donor ligand than its unsaturated analogue in this system, although the difference is less than was previously reasoned based on the notable enhancement of catalytic activity in the second generation olefin metathesis catalyst **3** (containing SIMes) when compared to **2** (containing IMes).[8−13] The Cp*Ru(L)Cl system has proven to be a good model for the ruthenium-based olefin metathesis system in terms of quantifying ligand effects and properties. The present data suggest that only small differences in the donor capabilities of NHC ligands might be responsible for significant catalytic enhancement in ruthenium olefin metathesis systems.

Experimental and Computational Details

General Considerations. All reactions were carried out using standard Schlenk techniques[48] under an atmosphere of dry argon or in an MBraun glovebox containing dry argon and less than 1 ppm oxygen. The syntheses of all ruthenium complexes described here required dry, degassed solvents, distilled from appropriate drying agents (pentane, toluene, and THF were distilled from sodium/benzophenone; hexane was passed through alumina columns of an MBraun solvent purification system). Other anhydrous solvents were purchased from Aldrich and degassed prior to use by purging with dry argon for 30 min. Solvents for NMR spectroscopy were dried under argon and transferred under vacuum into flame-dried Schlenk flasks from appropriate drying agents before use (THF, Na/K; C_6D_6, C_7D_8, sodium/benzophenone; CD_2Cl_2, $CDCl_3$, P_2O_5). $[Cp^*RuCl]_4$ was prepared according to the literature procedures.[49] NMR spectra were recorded on a 400 MHz Varian Gemini spectrometer.

Synthesis of Cp*Ru(SIMes)Cl (4). $[Cp^*RuCl]_4$ (200 mg, 0.18 mmol) and SIMes (226 mg, 0.74 mmol) were weighed into a 50 mL Schlenk flask, and THF (10 mL) was added. The resulting deep blue solution was stirred for 1 h, then the THF was removed in vacuo and the blue solid washed with pentane (2 × 5 mL) at −78 °C, affording 276 mg (69% yield) of the desired complex. Small crystals of X-ray quality were obtained by cooling a saturated pentane solution to −50 °C. Anal. Calcd for $C_{31}H_{41}ClN_4Ru$: C, 61.41; H, 6.83; N, 4.62. Found: C, 61.69; H, 6.59; N, 4.62. ^1H NMR (C_7D_8, 400 MHz): δ 6.74 (s, 2H, SIMes-4-C*H*), 6.65 (s, s, 2H, SIMes-4-C*H*), 3.20 (m, 4H, SIMes-NCH_2CH_2N), 2.50 (s, 6H, SIMes-CH_3), 2.29 (s, 12H, SIMes-CH_3), 2.08 (s, 6H, SIMes-CH_3), 1.11 (s, 15H, Cp*-CH_3). ^{13}C NMR (d_8-THF, 100.6 MHz): δ 229.18 (s, N-*C*-N), 139.43 (s, SIMes-*C*), 138.06 (s, SIMes-*C*), 136.91 (s, SIMes-*C*), 130.35 (s, SIMes-*C*), 129.50 (s, SIMes-*C*), 74.03 (s, Cp*-*C*), 52.03 (s, N*C*H_2*C*H_2N), 21.11 (s, SIMes-*C*H_3), 20.20 (s, SIMes-*C*H_3), 19.75 (s, SIMes-*C*H_3), 10.74 (s, Cp*-*C*).

Synthesis of Cp*Ru(SIPr)Cl (5). $[Cp^*RuCl]_4$ (200 mg, 0.18 mmol) and SIPr (288 mg, 0.74 mmol) were weighed into a 50 mL Schlenk flask, and THF (10 mL) was added. The resulting deep blue solution was stirred for 1 h at room temperature, then the THF was removed in vacuo and the deep blue solid extracted into pentane (50 mL). The pentane was removed to afford 109 mg (92% yield) of the blue crystalline complex. Crystals of **5** suitable for X-ray diffraction were obtained by cooling a concentrated pentane solution to −50 °C. Anal. Calcd for $C_{43}H_{69}N_2ClRu$: C, 68.81; H, 9.27; N, 3.73. Found: C, 69.22; H, 9.16; N, 3.87. ^1H NMR (C_6D_6, 400 MHz): δ 7.17 (m, 6H, SIPr-3-*H*), 3.95 (hept, $^3J_{HH} = 7$ Hz, 2H, ^{i}Pr-C*H*), 3.84 (hept, $^3J_{HH} = 7$ Hz, 2H, ^{i}Pr-C*H*), 3.52 (m, 4H, NCH_2CH_2N), 1.58 (d, $^3J_{HH} = 7$ Hz, 6H, ^{i}Pr-CH_3), 1.54 (d, $^3J_{HH} = 7$ Hz, 6H, ^{i}Pr-CH_3), 1.18 (d, $^3J_{HH} = 7$ Hz, 6H, ^{i}Pr-CH_3), 1.16 (s, 15H, *H*-Cp*), 1.05 (d, $^3J_{HH} = 7$ Hz, 6H, ^{i}Pr-CH_3). ^{13}C NMR (d_8-THF, 100.6 MHz): δ 232.27 (s, N*C*N), 150.17 (s, SIPr-*C*), 146.43 (s, SIPr-*C*), 138.35 (s, SIPr-*C*), 128.96 (s, SIPr-*C*H), 125.30 (s, SIPr-*C*H), 123.21 (s, SIPr-*C*H), 73.81 (s, Cp*-*C*), 53.87 (s, N*C*H_2*C*H_2N), 28.70 (s, SIPr-*C*H_3), 28.08 (s, SIPr-*C*H_3), 27.04 (s, SIPr-*C*H_3), 26.81 (s, SIPr-*C*H_3), 25.59 (s, SIPr-*C*H_3), 23.53 (s, SIPr-*C*H_3), 10.82 (s, Cp*-*C*H_3).

Computational Details

DFT Calculations. Geometries of the Cp*Ru(L)Cl complexes were optimized with the Amsterdam Density Functional (ADF) program.[50−53] The electronic configurations of the molecular systems were described by a triple-ζ STO basis set on ruthenium for 4s, 4p, and 4d, augmented with a 5p polarization function (ADF basis set TZP).[50] Triple-ζ STO basis sets were used for chlorine (3s,3p), nitrogen and carbon (2s,2p), and hydrogen (1s), augmented with two 3d, 3d, and 2p functions, respectively (ADF basis set TZ2P).[50] Inner shells on ruthenium (including 3d), chlorine (including 2p), and nitrogen and carbon (1s) were treated within the frozen core approximation. Energies and geometries were evaluated by using the local exchange−correlation potential by Vosko et al.,[54] augmented in a self-consistent manner with Becke's[55] exchange gradient correction and Perdew's[56] correlation gradient correction. Relativistic effects were included self-consistently in the geometry optimizations with the zero-order regular approximation (ZORA keyword in ADF).[57] Since relativistic effects were included, the TZP and TZ2P ZORA basis sets of ADF were utilized.[50]

Acknowledgment. We gratefully acknowledge the National Science Foundation and the Board of Regents of the State of Louisiana for generous financial support for this project. L.C. thanks the financial support of MURST of Italy (Grant PRIN-2002) and of the CIMCF of the Università Federico II of Naples for technical support.

Supporting Information Available: Tables of crystal data and structure refinement, atomic coordinates, bond lengths and angles, anisotropic displacement parameters, and hydrogen coordinates for complexes **4** and **5**, and the DFT Cartesian coordinates of all the structures discussed. This material is available free of charge via the Internet at http://pubs.acs.org.

OM034016K

---

(48) Errington, R. J. *Advanced Practical Inorganic and Metalorganic Chemistry*; Chapman and Hall: Bury St. Edmunds, 1997.

(49) Fagan, P. J.; Ward, M. D.; Calabrese, J. C. *J. Am. Chem. Soc.* **1989**, *111*, 1698−1719.

(50) *ADF 2000.03, Users's Manual*; Vrije Universiteit Amsterdam: Amsterdam, The Netherlands, 2002.

(51) Baerends, E. J.; Ellis, D. E.; Ros, P. *Chem. Phys.* **1973**, *2*, 41−51.

(52) te Velde, G.; Baerends, E. J. *J. Comput. Phys.* **1992**, *99*, 84−98.

(53) te Velde, G.; Bickelhaupt, F. M.; Baerends, E. J.; Fonseca Guerra, C.; Van Gisbergen, S. J. A.; Snijders, J. G.; Ziegler, T. *J. Comput. Chem.* **2001**, *22*, 931−967.

(54) Vosko, S. H.; Wilk, L.; Nusair, M. *Can. J. Phys.* **1980**, *58*, 1200−1211.

(55) Becke, A. *Phys. Rev. A* **1988**, *38*, 3098−3100.

(56) (a) Perdew, J. P. *Phys. Rev. B* **1986**, *33*, 8822−8824. (b) Perdew, J. P. *Phys. Rev. B* **1986**, *34*, 7406.

(57) van Lenthe, E.; Snijders. J. G.; Baerends, E. J. *J. Chem. Phys.* **1996**, *105*, 6505−6516.